

Chapter 4

Structural Studies

Transmission Electron Microscopy

&

Scanning Electron Microscopy

4.1 Characterization Techniques

4.1.1 Transmission Electron Microscopy (TEM)

Transmission electron microscopy (TEM) is a microscopy technique where a beam of electrons is transmitted through an ultra thin specimen, interacting with the specimen as it passes through. An image is formed from the interaction of the electrons transmitted through the specimen; the image is magnified and focused onto an imaging device, such as a fluorescent screen, on a layer of photographic film, or to be detected by a sensor such as a CCD camera. TEM Characterization of our samples were carried out at two different facility centres during our research work. One at UGC-CSR, Indore centre and other at SICART, Vidhyanagar. Images of TEM instrument at both centers are shown below.

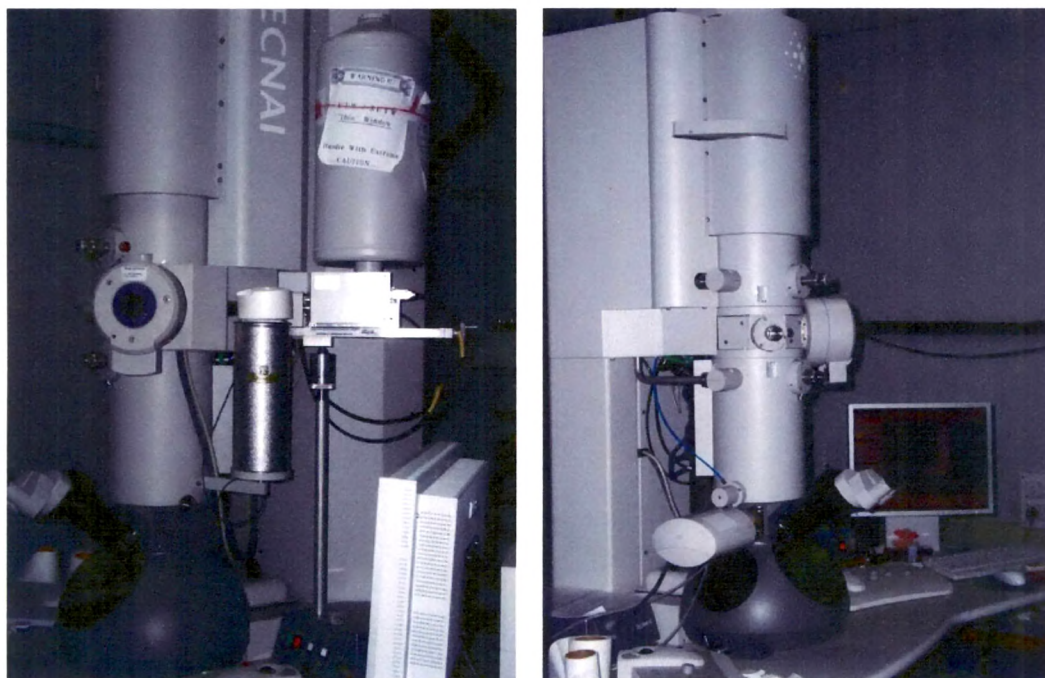


Figure 4.1 Photograph of TEM (Model : Philips Tecnai 20 G2, FEI make) instrument at UGC-CSR, Indore Centre.

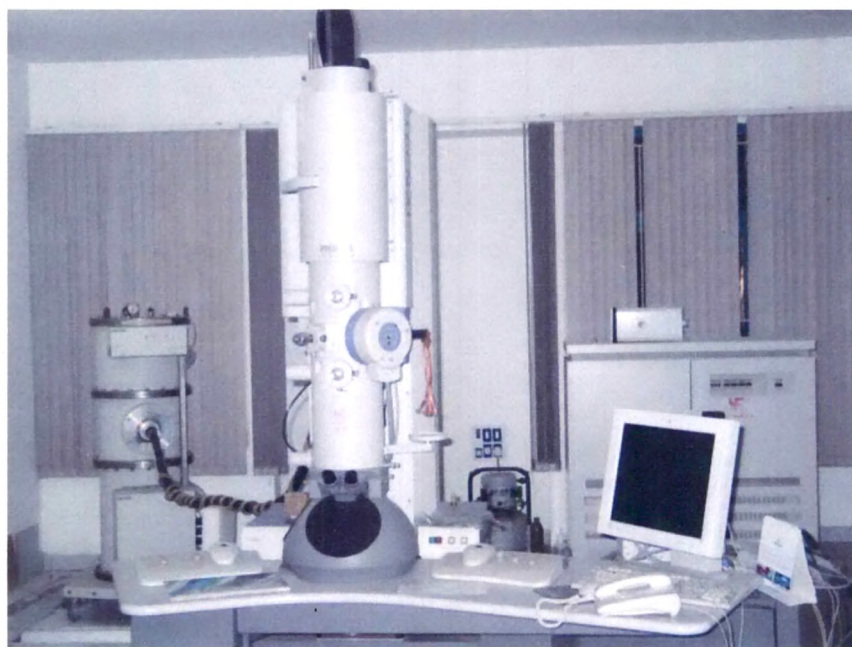


Figure 4.2 Photograph of TEM (Model : Philips Tecnai 20, Holland) instrument at SICART, Vidhyanagar, Anand.

4.1.2 Scanning Electron Microscopy (SEM)

Scanning electron microscopy (SEM) is a type of electron microscopy that images a sample by scanning it with a beam of electrons in a raster scan pattern. The electrons interact with the atoms that make up the sample producing signals that contain information about the sample's surface topography, composition, morphology, shape and size. Preparation of the samples is relatively easy since most SEMs only require the sample to be conductive. The SEM has a large depth of field, which allows a large amount of the sample to be in focus at one time. The SEM also produces images of high resolution, which means that closely spaced features can be examined at a high magnification. SEM characterization of our samples were carried out at Electrical Research Development Association (ERDA), Vadodara.

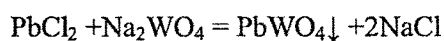
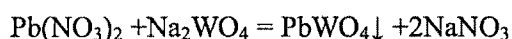
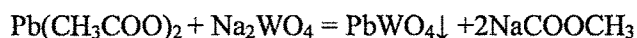


Figure 4.3 Photograph of SEM (JEOL JSM-6380LV) instrument at ERDA, Vadodara.

4.2 Introduction

It is well known that the crystal growth is controlled by the extrinsic as well as intrinsic factors, including the degree of supersaturation, diffusion of the reaction, surface energy, crystal structure etc. in the solution reaction system. Crystallization process can be divided into two events: *Nucleation* and *Crystal growth*. The size and the morphology of the products depend on the competition between nucleation and crystal growth, which are determined by the inherent crystal structure and the chemical potential in the precursor solution.

In our experiments PbWO_4 were synthesized in aqueous solution under the effect of different reaction conditions i.e. Pb Source, temperatures, pH of reaction solution. As a result, we obtained undoped and Cerium PbWO_4 nanomaterials through the reaction between Pb^{2+} and WO_4^{4-} at hydrothermal conditions having interesting morphologies. In present work, we have not used any type of directing or capping agent e.g. CTAB, PVP, EG etc. because these surfactants are expensive which increase the production cost. The reaction processes can be expressed as follows:



By mixing Na_2WO_4 and surfactant (distilled water in our case), $(\text{WO}_4)^{2-}$ anions were possibly coordinated to the surfactant molecules to form surfactant-tungstate complexes. The addition of Lead source compound into the solution containing the surfactant-tungstate complexes under the assistance of constant magnetic stirring and heating in Teflon lined Stainless steel autoclave led to the substitution of the surfactant by Pb^{2+} cations. At the beginning of the reaction, PbWO_4

nuclei produced in solution aggregate to form small particles. These particles may serve as crystal seeds to grow the building blocks for different structures. Once PbWO_4 nuclei (very fine particles) formed, they came together to form crystalline solids. The surfactant may have been selectively adsorbed onto the crystals and possibly desorbed due to magnetic stirring and heating in autoclave, resulting in a particular shape from the anisotropic process.

4.3 Effect of Lead Source on Morphology of PbWO₄

As discussed in Section 3.3.2 of Chapter 3, large single crystals of PbWO₄ are extensively grown using PbO and WO₃ as precursors which were used for scintillation detector or other application based on macro dimensions. Recent development in nanotechnology requires PbWO₄ material having different morphologies and dimensions suitable for nano-devices. So it is important to study effect of different reaction parameters (Precursor, pH, Concentration, Time and Temperature) on morphology of the final product. Among these effect of reaction parameters pH, concentration, time and temperature had reported in many literatures. It should be noted that the effect of different Lead sources on morphology and crystal structure of PbWO₄ has not been investigated yet except us [1]. Lead sources (Lead Acetate, Lead Nitrate and Lead Chloride) have different chemical properties and hence react differently with Na₂WO₄ under the same hydrothermal reaction conditions. They required different amount of energy in order to react with Na₂WO₄ rather surfactant-tungstate complex to form PbWO₄. The effect of different Lead sources [Pb(CH₃COO)₂, Pb(NO₃)₂ and PbCl₂] on the morphology of PbWO₄ were investigated from TEM and SEM characterization. Many interesting morphologies were produced in our experiments without the use of expensive template or surface directing capping agents by facile low temperature hydrothermal method. The results of our experiments demonstrate that different Lead sources could also affect the morphology of the products as discussed below.

4.4 PbWO₄ prepared with Lead Acetate

The morphology of pure and Cerium doped PbWO₄ prepared by Pb(CH₃COO)₂ (Lead Acetate) as a lead source were characterized through SEM and TEM. When Pb(CH₃COO)₂ was used as the Lead source, obtained PbWO₄ displayed agglomerated dendrite or seaweed like shape of around 5 μm [see Figure 4.4(b)] long and regular tetrahedron shaped particles are about 500nm size [see Figure 4.4(d)]. Dendrites are well-defined, complex and highly ordered and structurally similar to those prepared by sonochemical preparation method with N-cetyl pyridinium chloride surfactant [2] shown in Figure 4.4(a). The individual PbWO₄ dendrite shown in inset of Figure 4.4 (a) and (b) has only one trunk and shrunken branches. The branches are perpendicular to the trunk and they are built up of parallel-arrayed particles.

4.4.1 Tetrahedron shaped microparticles of PbWO₄

Small crystalline nuclei are formed in a highly supersaturated solution right after the mixing of the reactants at the molecular level called nucleation process. These tiny nuclei acted as precursor to form various morphologies. Thermodynamically all of the nuclei will grow towards the shape having the lowest energy at equilibrium. Larger particles grew at the cost of the small ones, due to the difference in solubility between the large particles and the small particles according to Gibbs-Thomson law. Synthesis of such type of tetrahedron shaped particles was reported by Qilin Dai et al in [3] by hydrothermal method. These crystals further aggregate and attach to each other by oriented attachment process to form dendrite shaped microstructures. Moreover, The Ostwald ripening process contributes to the self-assembly of the tetrahedron nanocrystals by sharing the edges of polyhedrons.

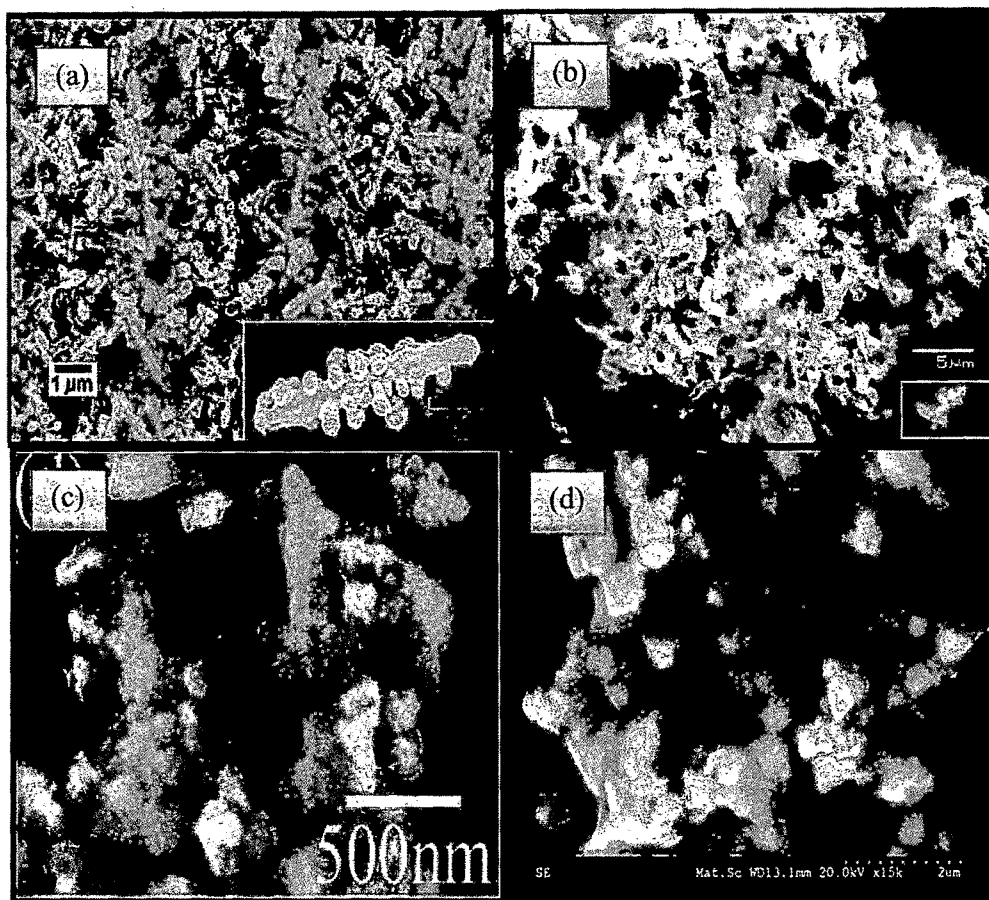


Figure 4.4 SEM images of PbWO_4 (a) agglomeration of dendrite with single trunk reported in ref. [2]; (b) single trunk dendrite produced using Lead Acetate as lead source; (c) tetrahedron microparticles reported in ref. [3]; (d) tetrahedron microparticles produced using Lead Acetate as lead source.

4.5 PbWO₄:Ce prepared with Lead Acetate

According to literature survey only Yan Fang et.al. [4] reported the effect of Ce doping on morphology of PbWO₄ produced using Lead Acetate as Lead source. He found that Cerium doping in PbWO₄ changes morphology from Prism-like structure with terminating pyramids to shuttle shape. Similar type of Prism-like morphology (Tetrahedron microparticles) of undoped PbWO₄ also produced in our case as mentioned in previous section but when Cerium was doped one dimensional microbelts like morphology was obtained shown in Figure 4.5 and Figure 4.6. Possible reason and process for production of microbelt like structure is explained in detail in the next section.

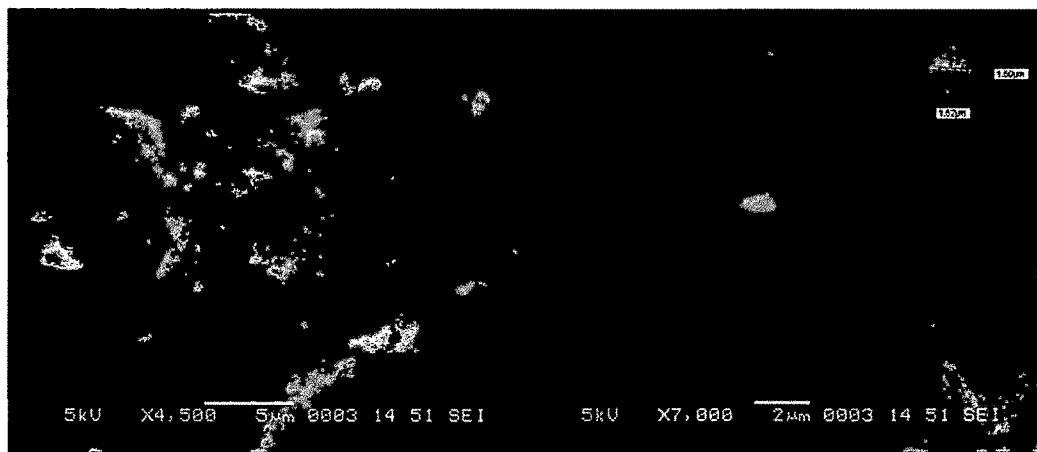


Figure 4.5 SEM images of microbelts (left) and octahedron microparticles (right) of PbWO₄:Ce produced using Lead Acetate as lead source.

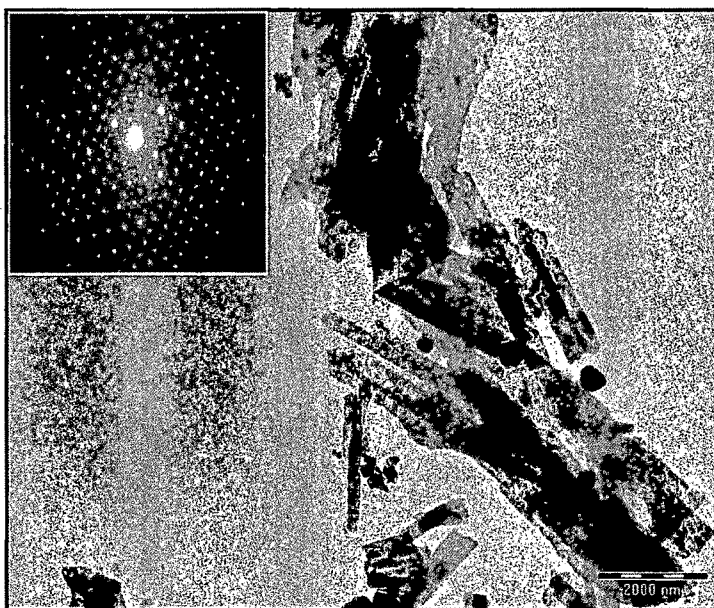


Figure 4.6 TEM images of $\text{PbWO}_4:\text{Ce}$ produced using Lead Acetate as lead source.

Figure 4.5 represents the SEM photographs of Cerium doped PbWO_4 prepared by Lead Acetate as a lead source. As shown in images Cerium doping in PbWO_4 host lattice produced flat microbelt. $\text{PbWO}_4:\text{Ce}$ microbelts are about $5\mu\text{m}$ long and about $1\mu\text{m}$ broad. High magnification SEM image [Figure 4.5 (right)] shows that Octahedron shaped Cerium doped PbWO_4 microparticles are also present along with microbelt. An individual $\text{PbWO}_4:\text{Ce}$ Octahedron particle is shown in inset of Figure 4.5 (right) having length along the long axis about $1.52\mu\text{m}$ and along short axis about $1.50\mu\text{m}$. Formation of such microbelt like structures also supported by TEM photograph as shown in Figure 4.6 TEM image inferred agglomeration of microbelts having width about 100nm and few μm in length. Electron Diffraction (ED) pattern of thus obtained PbWO_4 is shown in inset of Figure 4.6. ED patterns shows well crystalline microbelts were formed at low temperature mild hydrothermal method.

4.5.1 Raspite Phase

In ref. [1] we have proposed that one dimensional flat microbelt like structure is produced due to raspite phase of PbWO_4 . Cerium will not play any direct role in the production of belt like structure. Very few reports have been published on the preparation of raspite phase in the laboratory. The raspite PbWO_4 nanobelts were synthesized using charged dextran as a structure directing coordination molecular template by J.Yang [5]. With the assistance of PVP surface-capping agent, the bamboo-leaf-like raspite PbWO_4 nanostructures were fabricated by T. Gorge et al [6] and with composite-salt-mediated synthesis method by C. Zheng [7] to prepare ultra-long PbWO_4 raspite nanobelts. C. Zheng prepared few millimetre long PbWO_4 nanobelts at 160°C for 18 h reaction duration by using composite-salt ($\text{LiNO}_3/\text{KNO}_3$) at 9 pH while we get PbWO_4 nanobelts about $5\mu\text{m}$ long and 500 nm broad at comparatively low (100°C) temperatures for short (12h) reaction time at 7pH. This result shows that PbWO_4 microbelts can be produced at lower temperature without using any surfactant/capping agent or composite salt by hydrothermal method. Morphology of PbWO_4 microbelt produced in our case is similar to bamboo-leaf- like which is close to reported by T.Geogre et al. using polyol (polyethylene glycol-200).

4.5.2 Growth Mechanism of PbWO₄ microbelt

A schematic illustration of the growth mechanism of the raspite phase lead tungstate microbelt is shown in Figure 4.7. In the initial stage, the OH⁻ ions from H₂O react with Pb²⁺ ions of Lead Source to produce the Pb(OH)₂ molecule. The Pb(OH)₂ molecule further reacts with (WO₄)²⁻ ion of Na₂WO₄ to form PbWO₄ nuclei and release OH⁻ ions, and the latter is adsorbed on the surface of the former.

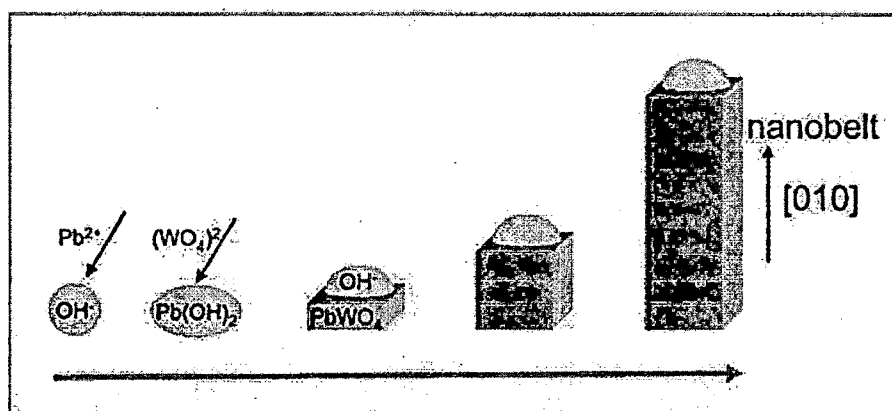


Figure 4.7 Growth mechanism of PbWO₄ microbelt suggested by C. Zheng [7].

In the second stage, the adsorbed OH⁻ ion reacts with a nearby Pb²⁺ ion to produce Pb(OH)₂, and then react with (WO₄)²⁻ ions to form the bigger PbWO₄ nuclei. Unit cell of raspite PbWO₄ contain four Pb²⁺, four W⁶⁺ and sixteen O²⁻ ions. Table 4.1 shows calculated atomic packing density for different faces for different lead sources.

Table 4.1 Summary of lattice parameter and atomic packing density of different lead sources.

Lead Source	Lattice Parameter (Å)			Atomic packing density (Å ⁻²)		
	a	b	c	(100)	(010)	(001)
Lead Acetate	13.525	4.9682	5.546	0.036	0.028	0.030
Lead Nitrate	13.580	4.9900	5.5600	0.036	0.028	0.030
Lead Chloride	13.555	4.9760	5.5601	0.036	0.028	0.030

Due to the structured anisotropy of the raspite PbWO_4 crystal, the top faces (exposure surfaces) of (100), (010) and (001) have different atomic packing density and surface energy. Theoretically, the face that contains all four Pb^{2+} ions possesses the highest density of Pb^{2+} ions, though this kind of face is unusual and less stable. The density of Pb^{2+} ions in this face is about 0.045 \AA^{-2} . However, the density of possible exposure surfaces calculated is 0.036 \AA^{-2} [$1/(4.968 \text{ \AA} \times 5.546 \text{ \AA})$] for (100), 0.028 \AA^{-2} [$2/(13.52 \text{ \AA} \times 5.546 \text{ \AA} \sin 107.7^\circ)$] for (010) and 0.030 \AA^{-2} [$2/(13.52 \text{ \AA} \times 4.968 \text{ \AA})$] for (001) faces. Atomic packing density is inversely proportional to the surface energy. In other words, the top faces (exposure surfaces) of (100) and (001) of PbWO_4 nanobelts may have larger packing density and lower surface energy, while the top faces of (010) have the smallest packing density and highest surface energy [8]. So the OH^- ions would be preferentially adsorbed on the (010) faces to reduce the surface energy, which finally form the quasi-one-dimensional PbWO_4 microbelts after periodical repeat of the previous growth process. So it is reasonable to conclude that the PbWO_4 microbelt grows along the [010] direction to reduce surface energy with the side faces of the microbelt contained by the Pb^{2+} -enriched (100) and (001) planes. Similar type of PbWO_4 microbelts also produced when we use $\text{Pb}(\text{NO}_3)_2$ and PbCl_2 as lead sources, which shows that the process of PbWO_4 microbelt formation is independent of Lead Sources.

4.6 PbWO_4 prepared with Lead Nitrate

PbWO_4 was synthesized using Lead Nitrate as a Lead source. When $\text{Pb}(\text{NO}_3)_2$ was used as the lead source, the product consists of agglomerated microbelts and dendrites as we can see from SEM images in Figure 4.8. Microbelts are flat with irregular edge. Average length of microbelt is about $5\mu\text{m}$ and width is about $1\mu\text{m}$. Similar type of microbelts with regular edges were also produced in the case of Cerium doped PbWO_4 synthesized using Lead Acetate. Dendrite having single trunk were produced with Lead Acetate while here three dimensional dendrites having six branched or trunk is produced. The length of the long trunk is about $2.10\mu\text{m}$ and that of the two branches is about $1.18\mu\text{m}$ can be seen in inset of Figure 4.8 (b).

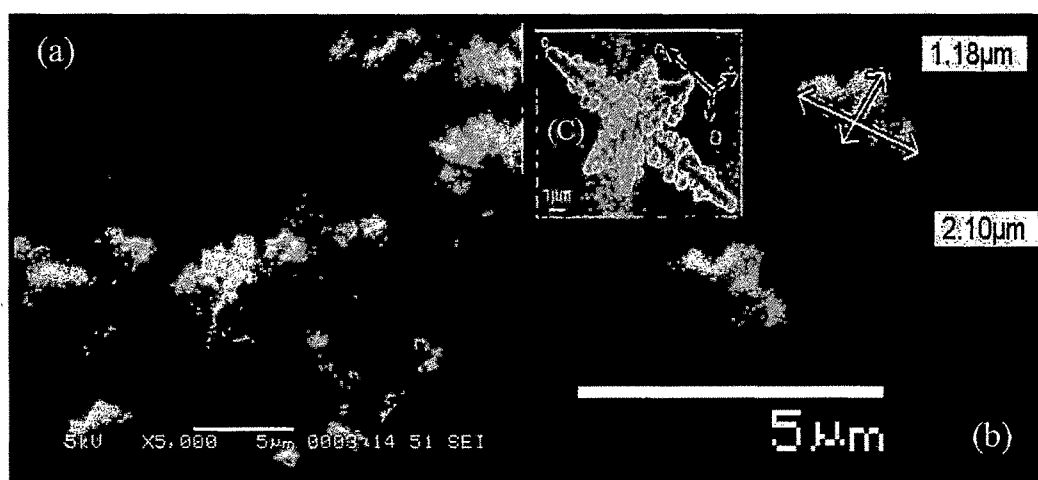


Figure 4.8 (a) SEM image of agglomerated microbelts and dendrites of PbWO_4 ; (b) High magnified SEM image of individual six branched/trunk dendrite (inset shows same dendrite with scale); (c) Three dimensional dendrite reported in [9] by Biao Liu et al. with CTAB surfactant.

4.6.1 Explanation of formation of PbWO_4 3-Dimensional dendrite

However, the individual PbWO_4 dendrite with three-dimensional structure displays more complex features which are similar to reported by Biao Liu et al. with CTAB surfactant with Hydrothermal method [9] as shown in a higher magnification SEM image of individual dendrite (inset to Figure 4.8 (c)). 3-dimensional dendrite structure is complex, uniform and systematic. There are two pair of short trunks and one pair of long trunk. The trunks are in the shape of pine trees and have arrowhead-shaped tips. Four branches of two short trunks grow vertically on main long trunk in perpendicular directions and in the same plane. The length of the long trunk is about $2.10 \mu\text{m}$ and that of the two paired branches is about $1.18 \mu\text{m}$. The ratio of the lengths of the three main trunks is equal to the ratio of the cell parameters $c/a = c/b = 2.2:1$; therefore, it is believed that the longer trunk grew in the c direction and the two shorter ones, in a or b directions. PbWO_4 dendrite produced in our case is 10 times smaller than that of reported by Biao Liu et. al. We have not used expensive surface capping agent to produce such a 3-dimensional structure which lowers the production cost though optimisation is required. The dimensions of such high hierarchical structures finely reflect the intrinsic cell structure of stolzite. Further optimization of the growth conditions could make it possible to obtain perfect uniform hierarchical structures.

4.6.2 Explanation of formation of rhombic shaped PbWO_4 particles

PbWO_4 particles with rhombic shape were also produced with Lead Nitrate which is shown in Figure 4.9 (a) of below TEM image.

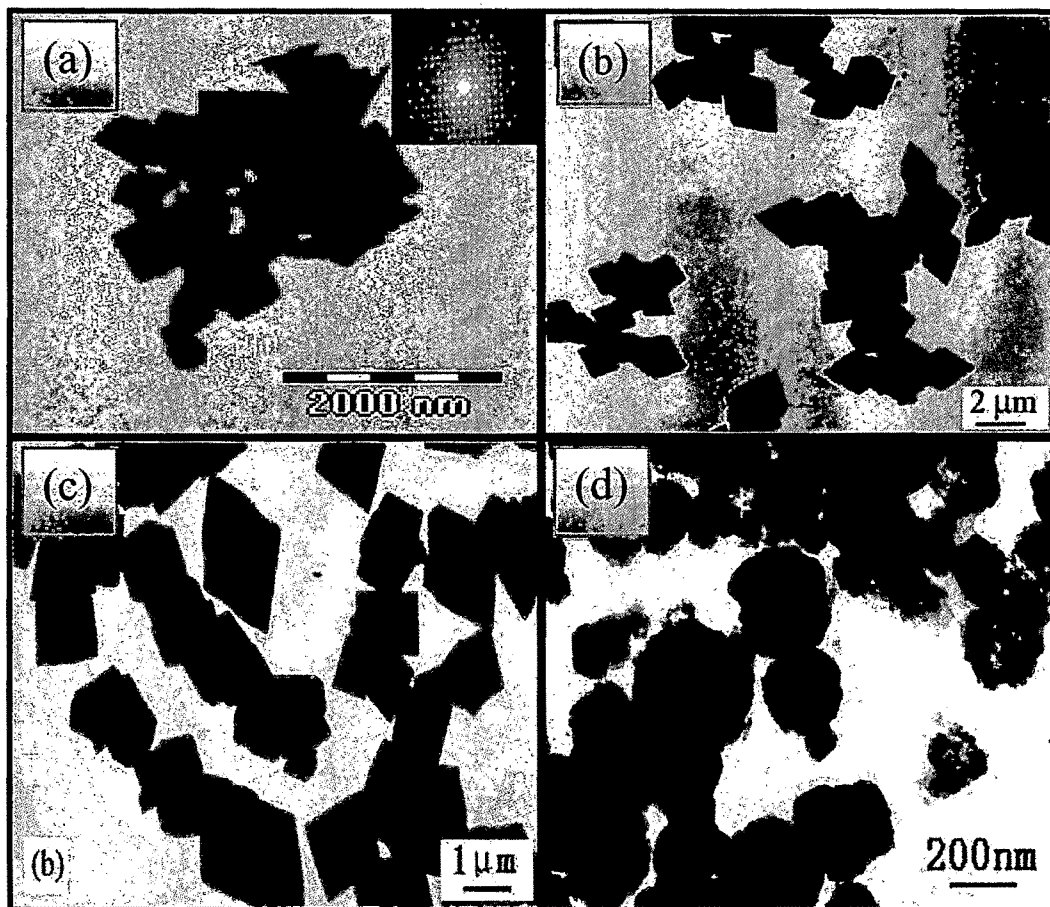


Figure 4.9 TEM image of rhombic shaped PbWO_4 microparticles (a) synthesized by us without using any surfactant; (b) synthesized by using PVP [12] and (c) CTAB [13] surfactant; (d) nanoparticles prepared without surfactant.

As mentioned earlier, the PbWO_4 nanoparticles are produced via hydrothermal crystallization process in the supersaturated solution. One basic crystal-growth mechanism in supersaturated solution systems is the well known “Ostwald ripening process” [10]. In the Ostwald ripening process, the initial formation of tiny crystalline nuclei in a supersaturated medium is followed by crystal growth. In this process the larger particles grow at the cost of the small ones due to the energy difference between large particles and small particles. This difference is reflected in the higher solubility of the smaller particles as defined by the Gibbs–Thompson law [11] which tells that solubility is inversely proportional to the particle size. These freshly formed nuclei are unstable and have the tendency to grow into larger particles due to their high chemical potential. The rhombic-shaped particles are then formed via a transformation process using the PbWO_4 nanoparticles [Figure 4.9 (d)] as precursors. Guangjun Zhou et al. had produced similar shaped PbWO_4 micro sized particles by using PVP (poly-vinyl-pyrrolidone K30) [12] and CTAB [13] (cetyltrimethylammonium bromine) shown in Figure 4.9 (b) and (c), respectively. It should be noted that we have not use any type of surfactant to produced rhombic shaped PbWO_4 . Moreover PbWO_4 particle which are produced in our experiments are about 500 nm in size while those prepared by Guangjun Zhou [12, 13] et al. are about 1 μm in size. This result shows that by using hydrothermal method we can produce rhombic shaped PbWO_4 without using any surfactant.

As reported by Changhua An in [14], rod and flake like morphology with stolzite phase of PbWO_4 was produced during 100-150 °C temperature range and 3-8 h reaction time, while in our case six branched dendrite, microbelt and rhombohedral morphology were produced around 100°C for 12 h reaction period. Comparing all the results we can say that initially nanoparticles are formed as soon as the both reactants

mixed in the supersaturated aqueous solution. When such mixture is treated in the autoclave for 3-8 hr PbWO_4 nanoparticles grow to form rod and flake like structure for shorter duration of reaction time. If we increase the reaction time for 12 h as in our case, rhombic shaped PbWO_4 microparticles are produced which turns into single or multiple branched dendrite or flat microbelt structure. Also we can conclude that at lower temperature raspite phase is produced and with increases in temperature raspite phase turns into stolzite phase.

4.7 PbWO₄:Ce prepared with Lead Nitrate

Preparation of Cerium doped PbWO₄ using Lead Nitrate as a Lead source is not reported yet by any other method except us with hydrothermal method [1]. Figure 4.10 shows TEM image of tetrahedron shaped microparticles of Cerium doped PbWO₄ at different magnification. Similar tetrahedron microparticles having size about 500nm were produced when Lead Acetate was used as Lead source. Size of microparticles is reduced to 100 nm which may attribute to smaller ionic radius of Ce³⁺ ion (0.103 nm) compared to Pb²⁺ ions (0.120 nm).

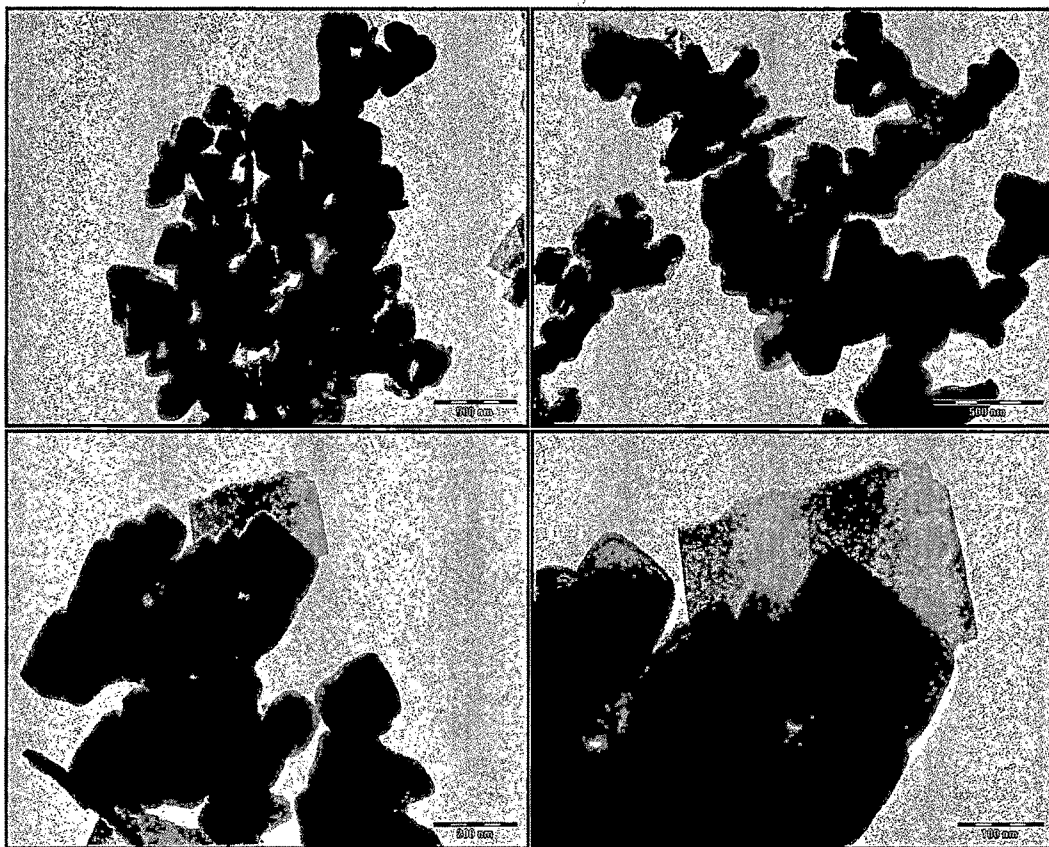
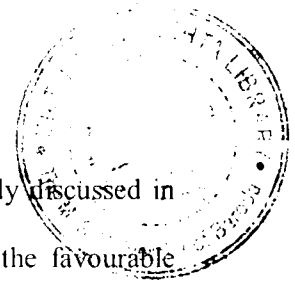


Figure 4.10 TEM images of Cerium doped tetrahedron PbWO₄ prepared using Lead Nitrate as a Lead source with different magnification.



Formation mechanism of Tetrahedron microparticles have been already discussed in section 4.4.1. The formation of PbWO_4 tetrahedron is attributed to the favourable thermo-dynamic conditions. The formation and evolution processes can be divided into three steps: initial nucleation process in supersaturated solution, self-assembly process (oriented aggregation), and subsequent crystal growth process (Ostwald ripening).

4.8 PbWO₄ prepared with Lead Chloride

According to our literature survey, only one paper by Changhua An [14] had been reported so far in which Lead Chloride was used as a Lead source to produce PbWO₄. PbWO₄ nanomaterial prepared with Lead chloride a Lead source shows excellence Photoluminescence compared to other that prepared with Lead Nitrate and Lead Acetate which will discussed in next chapter. The TEM photographs of PbWO₄ obtained by using Lead Chloride as a Lead source under identical reaction conditions shown in Figure 4.11. As shown in TEM images, microparticles of octahedron shape having size around 100 nm as well as flat microplates having width 100-150nm and about few μm in length are obtained. Changhua An et al. reported formation of similar type morphology for 100°C -150°C reaction temperature and 3-8 h reaction duration.

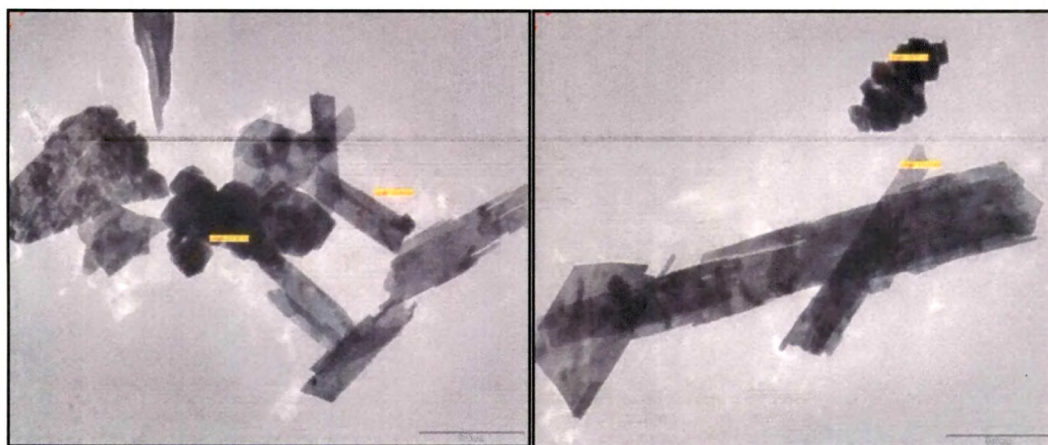


Figure 4.11 TEM images of agglomerated octahedron microparticles and flat micro belts of PbWO₄ prepared with Lead Chloride (both images are of same sample).

4.9 PbWO₄:Ce prepared with Lead Chloride

Cerium doping during preparation of PbWO₄, produces tetrahedron shaped microparticles having size around 100 nm as shown in Figure 4.11. Similar type of Tetrahedron shaped microparticles were produced with Lead Nitrate as a Lead source. Formation mechanism of PbWO₄ microparticles can explain on the basis of Oswald ripening process followed by oriented attachment of PbWO₄ microparticles to form dendrite like structure similar to that form in Lead Nitrate case.



Figure 4.12 TEM images of agglomerated tetrahedron microparticles of Cerium doped PbWO₄ prepared with Lead Chloride (both images are of same sample).

X-ray diffraction studies in the previous chapter 3 reveals that Cerium doping in the PbWO₄ crystal lattice suppress the formation of raspite phase and favours production of stolzite phase. We proposed that flat microbelt and flake like morphologies are related to raspite phase and dendrite (whether single or multiple branched), microparticles with tetrahedron and rhombic shaped morphologies are related to stolzite phase. As Cerium having tendency to suppress raspite phase related morphologies, morphologies related to stolzite phase predominantly produced in the Cerium doped samples. It should be noted that these type of behaviour is observed in

Cerium doped PbWO_4 samples prepared with Lead Nitrate and Lead Chloride. Cerium doped PbWO_4 samples prepared with Lead Acetate do not show this type of characteristics. Single branched dendrites (stolzite phase related morphology) produce in the case of undoped sample which is understood but Cerium doped sample produce microbelts (raspite phase related morphology) which is deviating our assumption. This contradiction can be explained on the basis of limitation of characterization techniques including skill of operating technician. We know that from xrd analysis, all the samples produced at 100°C temperature contains almost equal amount of stolzite as well as raspite phase. During TEM and SEM characterization very small areas of sample is focused. For example in the case of Cerium doped PbWO_4 , if the area being focused contains more amount of raspite phase related morphologies compared to stolzite one, we will get images of microbelts though remaining area of sample contains more amount of morphologies related to stolzite phase. It is our future aim to investigate in this direction by analysing Cerium doped PbWO_4 produced at higher temperatures by using Lead Acetate as a Lead source.

From above results we conclude that Cerium doping in PbWO_4 , tetrahedron shaped microparticles with stolzite phase is dominantly produced over raspite phase. Thus Cerium plays an important role in controlling the morphology of PbWO_4 prepared with Lead Nitrate and Lead Chloride. So we proposed that Cerium plays the role of surfactant or capping agent by regulating crystal growth direction. This is a very interesting phenomenon and it should be investigated for other types of rare earth elements also.

Thus we can see that various types of morphologies of undoped as well as Cerium doped PbWO_4 can be prepared by using different Lead sources. The results of above experiments are summarized in Table 4.2.

Table 4.2 Summary of morphologies and particle size of undoped and Cerium doped PbWO_4 prepared using different Lead sources.

Sample No.	Lead Source	Dopant	Morphology	Dimensions
1	$\text{Pb}(\text{CH}_3\text{COO})_2$	-	single branched dendrite	$1\ \mu\text{m}$
			tetrahedron	500nm
2	$\text{Pb}(\text{CH}_3\text{COO})_2$	CeO_2	flat nanobelt	$5\ \mu\text{m} \times 1\ \mu\text{m}$
			octahedron microparticles	$1.5\ \mu\text{m}$
3	$\text{Pb}(\text{NO}_3)_2$	-	flat nanobelt	$5\ \mu\text{m} \times 1\ \mu\text{m}$
			six branched dendrites	$2\ \mu\text{m}$
			rhombic microparticles	500nm
4	$\text{Pb}(\text{NO}_3)_2$	CeO_2	tetrahedron	100nm
5	PbCl_2	-	micro plates	few μm
			microparticles	100nm
6	PbCl_2	CeO_2	tetrahedron	100nm

4.10 Effect of reaction parameter on the morphology

Literature survey shows that reaction parameters such as pH of reaction solution during crystal growth, Temperature of reaction solution plays an important role to modified morphology and particle size of final product. In order to analyse effect of pH, Temperature and Cerium doping, TEM characterization of some selected samples are shown in below table were performed and discussed in this chapter.

Table 4.3 Summary of reaction conditions of undoped and Cerium doped PbWO_4 samples selected for TEM analysis.

Sample No.	PbCl_2 conc. (M)	Na_2WO_4 conc. (M)	Ce conc. (M)	Temp. ($^\circ\text{C}$)	Time (h)	pH
5	0.01	0.01	-	100	12	7
6	0.01	0.01	0.001	100	12	7
8	0.01	0.01	-	125	12	7
9	0.01	0.01	-	125	12	11
13	0.1	0.1	0.001	200	12	7

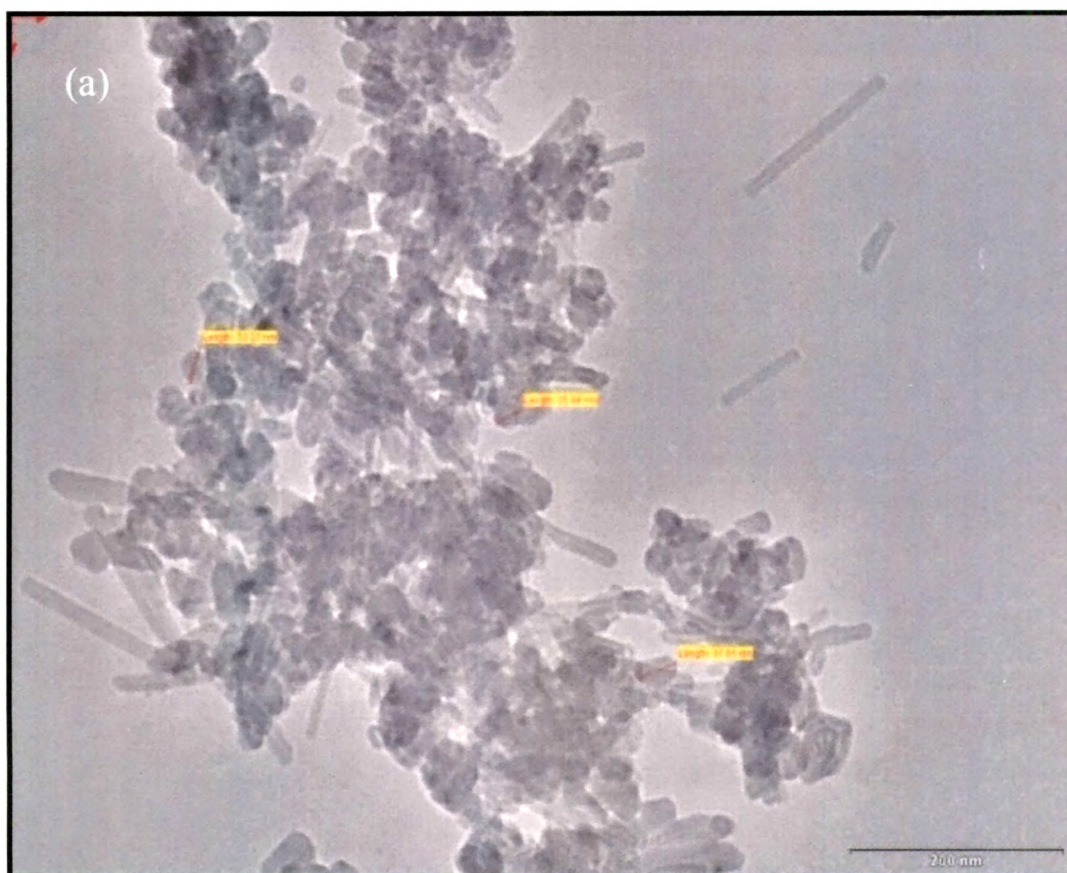
4.11 Effect of pH of reaction solution on morphology of PbWO₄

The pH value of reaction system is one of the most important factors. It has been found that the pH value of the precursor medium plays an important role in the formation of tungstate phase and its morphology. We assume that the influence of pH value on the growth of the PbWO₄ crystals may lie in three aspects: affecting the adsorption of surfactant to different facets, changing the relative energy of the different facets, and affecting the controlling growth mechanism.

As mentioned previously, we have prepared undoped PbWO₄ at three different pH values (3pH, 7pH and 11pH). X-ray diffraction analysis of these samples discussed in Chapter 3 shows that all three samples are highly crystallized and indexed to purely tetragonal stolzite phase. In order to analyze morphology of these samples with TEM, two samples (samples prepared at 7pH and 11pH) were chosen based on their excellent photoluminescence spectra. TEM images of PbWO₄ prepared at 7pH and 11pH are shown in Figure 4.13 and Figure 4.15, respectively. Both samples are prepared at 125 °C for 10 h reaction duration.

The product obtained at 7pH contains agglomerated Quasi-spherical hollow nanoparticles (HNPs) and hollow nanotubes (HNTs) of PbWO₄ as shown in Figure 4.13. Hollow Nanoparticle (HNPs) have an average diameter of about 20-40 nm and their shape is not perfectly spherical. PbWO₄ hollow nanotubes have outer diameter approximately 12.37 nm and length around 80-170 nm. Moreover, HNTs which are produced at 7pH are having uniform smooth surface. Upon rising pH to 11, nano particles were disappeared and bigger particles of irregular shape are formed as shown in Figure 4.16. PbWO₄ nanorods are also produced at 11pH but their length increases from 80-170 nm to 2µm with 40 nm outer

diameter. PbWO_4 nanorods produced at 11pH are not hollow like those formed at 7pH. Because of the small diameter, these nanorods have tendency to bundle together, a phenomenon always observed in single walled carbon nanotubes. A closer observation of the nanorods reveals that they have a narrow width distribution and uniform diameter throughout their entire length.



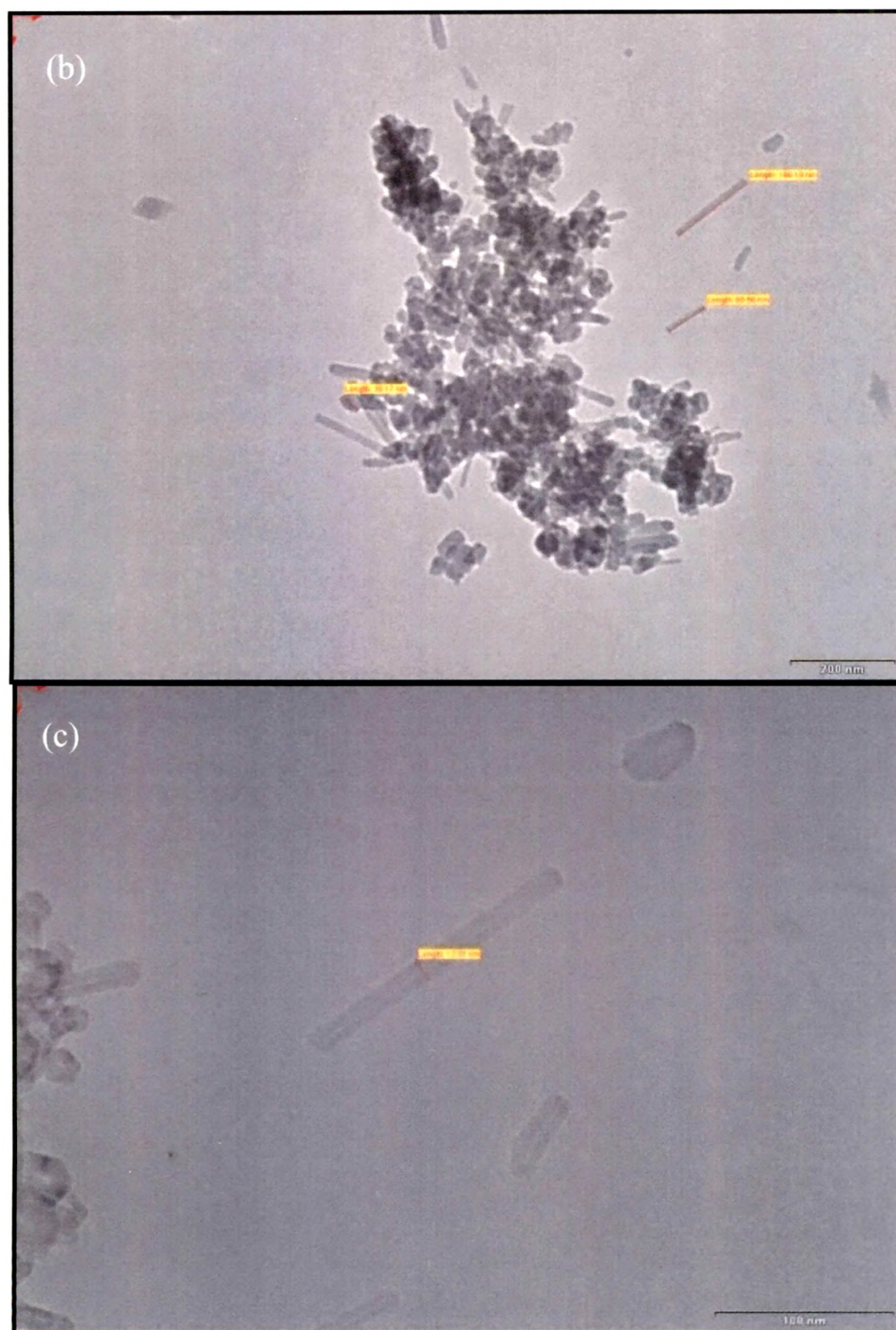


Figure 4.13 The high-magnification TEM images of (a) quasi-spherical hollow nano particles (HNPs) of PbWO₄ with scale (b) hollow nano tubes (HNTs) of PbWO₄ with scale (c) individual single HNT

4.11.1 Formation Mechanism of Hollow Nanostructures of PbWO_4

4.11.1.1 The Kirkendall Effect

The Kirkendall effect is a classical phenomenon in metallurgy [15-18]. It is basically refers to irreversible mutual diffusion process at interface of two metals compounds so that vacancy diffusion occurs to compensate for the inequality of the material flow and the initial interface moves. Prasad and Paul [19] derived the growth rate of the product layer as well as the rate of consumption of core and shell material. Following their formulation, it is possible to determine the radius of the core and shell, and time required to produce a single-phase nanotube.

4.11.1.2 Hollow Nanoparticles

Aldinger was the first to study the hollowing of spherical particles induced by the Kirkendall effect early in 1974 [21]. Only one author Fan Dong was reported the formation of hollow nano particles of PbWO_4 synthesized by ultrasonic spray pyrolysis method using citric acid surfactant. HNPs produced by them were bigger in size compared to us and have small pores on the surface while HNPs in our case has continuous surface. Formation of hollow nanoparticles (HNPs) in our case (Figure 4.13 (a)) can be explained on the basis of Kirkendall counter diffusion effect. This is a typical ternary compound reaction. In this reaction two reagents PbCl_2 (compound A) and Na_2WO_4 (compound B) sacrifice themselves to produce HNPs of PbWO_4 (compound AB). We proposed that there are two possible way: Process A and Process B. Both processes are based on Core/Shell model with difference only in Core and Shell Compound. Process A is shown schematically in Figure 4.14. In the Process A, (a) initially agglomerated PbCl_2 molecules behave as a Core and Na_2WO_4

molecules gathered around it and form a shell shown in **(b)**. Pb^{2+} ions from the core diffuse to the shell side and WO_4^{2-} ions from the shell diffuse to the core side. By this way Kirkendall diffusion will take place in the form of two way mass transfer (Wagner counter diffusion) between core and shell compounds. Thus the product PbWO_4 form at core/shell interface site. Simultaneously Na^+ move and react with Cl^- outer side to form NaCl which dissolve in aqueous solution. At the same time small isotropic voids are forms in core contains only Cl^- ions shown in **(c)**. Small Kirkendall voids merge into each other and forms larger cavities. If gaps are present at the core/shell interface which appear during the growth, Cl^- ions escape from these gaps and direct dissolution of Cl^- ions is taking place in solution phase shown in **(d)**, leading to hollowing of the PbWO_4 NPs shown in **(e)**. HNPs of PbWO_4 also form via Process B similar way with Na_2WO_4 as Core and PbCl_2 as Shell.

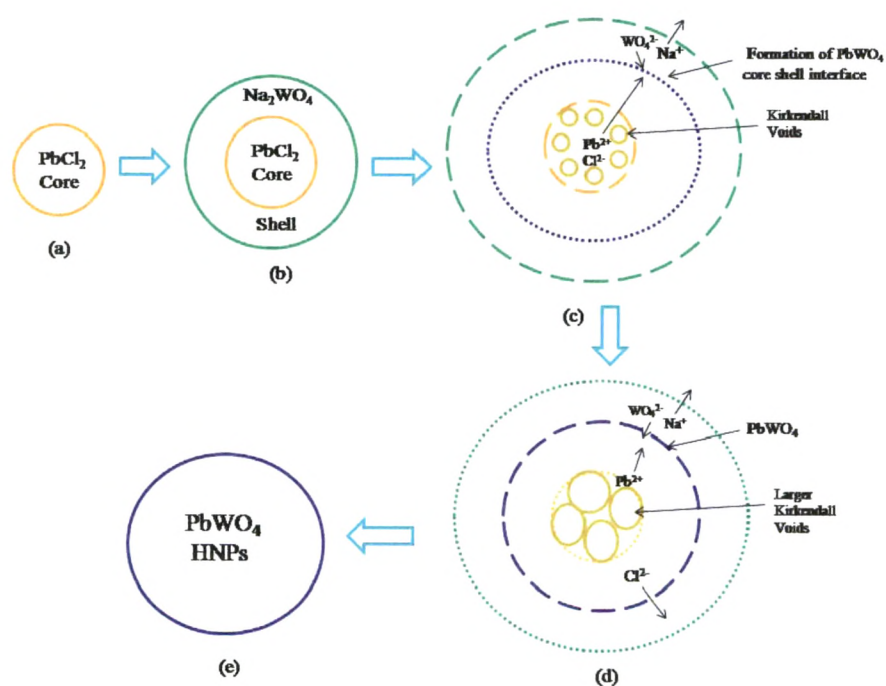


Figure 4.14 Schematic diagram showing formation of PbWO_4 Hollow Nano Particles by Process A.

4.11.1.3 Hollow Nanotubes

Formation of PbWO_4 Hollow Nano Tubes (HNTs) have not been reported yet, hence we are first to synthesis it. Formation tubular Hollow structures based on Kirkendall effect were reported in ref [21-28]. Ag_2Se nanotubes are shown in Figure 4.15 to compare it with HNTs PbWO_4 form in our case [29]. The Kirkendall-based formation route of PbWO_4 HNPs can also been extended to tubular structures as shown in Figure 4.13(c). The nanotubes have one more degree of freedom and allow material transport along the longitudinal axes. Elimination of the Cl^- from the core is taking place via open ends of Nanotubes which makes them hollow.

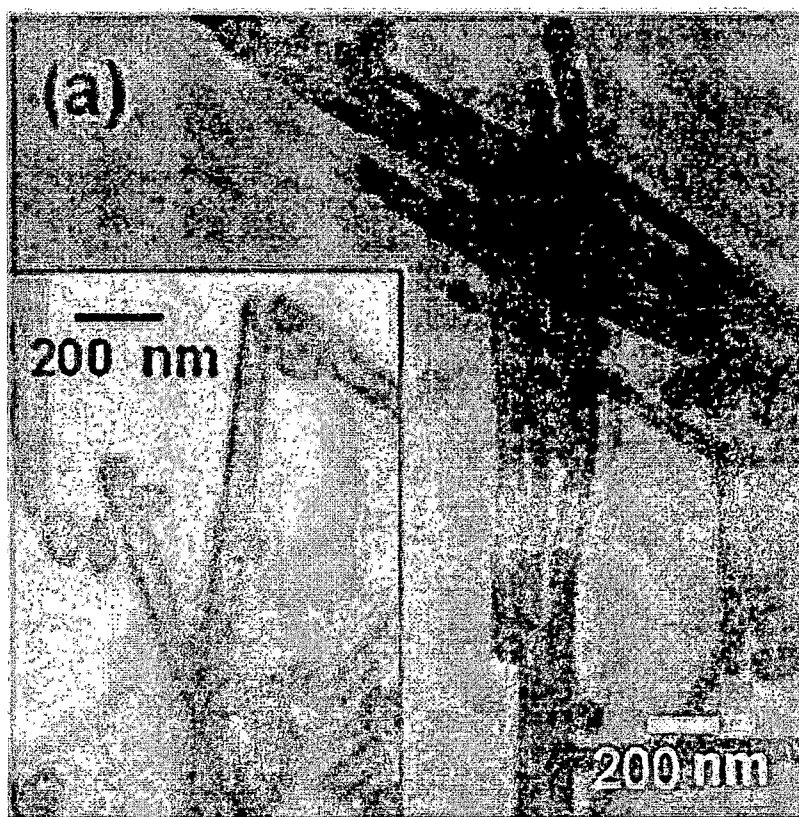


Figure 4.15 Polycrystalline Ag_2Se nanotubes [29]

From these observations, we can generally conclude that at 7pH, we get mixture of spherical Hollow nanoparticles which act as precursor and they gathered to form hollow nanotubes (HNTs). On increasing the pH of the precursor mixture, we obtained nanorods which are not hollow with increased length. From XRD and TEM analysis we can say that in the 7-11pH range highly crystallized 1-Dimensional PbWO_4 nanorods with pure stolzite phase obtained. These results indicate that this is the optimal pH range for the formation of PbWO_4 nanorods.

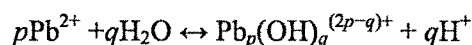


Figure 4.16 TEM image of agglomerated PbWO_4 nanorods

4.11.2 Formation Mechanism of 1-Dimensional PbWO₄ nanorods: Spherical Diffusion Model

The solid nanorods of PbWO₄ can be thought to be having a habit to form this morphology due to its crystal structures. Yu et al. [30] have recently reported the general synthesis of metal tungstate nanorods by the hydrothermal process without using templates or surfactants and found that the formation mechanism of the nanorods can be explained by the spherical diffusion model well. Anisotropic lateral growth of PbWO₄ nanorods can be explained by Sugimoto's spherical diffusion model [31].

According to spherical diffusion model there is a spherical diffusion layer of solute [Pb²⁺ or WO₄²⁻] around each crystal during lateral growth of PbWO₄ nanorods. Solubility is inversely proportional to particle size. As the particle size decreases solubility increases (Gibbs-Thompson law). The concentration of solute within the diffusion layer maintains the solubility of specific crystal face by rapid growth onto or dissolution from the face. The above surfactant\ ligand-free exclusive anisotropic growth of nanorods can be understood from the view point of intrinsic structure of the tungstates. At high pH e.g. at 11pH in our case, Pb²⁺ is extensively hydrolyzed [32, 33];



forming "mononuclear" ($p = 1$) and "polynuclear" ($p > 1$) species.

According to Peng et al [34] a higher monomer (Pb²⁺) concentration favors 1D-growth and lower monomer (Pb²⁺) concentration favours 3D-growth. At high pH, Pb²⁺ exists as Lead hydroxide complex Pb_p(OH)_q^{(2p-q)+} instead of PbWO₄, which Lead to a relatively slow release of Pb²⁺ and lower Pb²⁺ concentration, which result in the formation of larger PbWO₄ particles.

At pH 7 reaction system could provide a higher monomer (Pb^{2+}) concentration due to the relatively weaker metal complexing association and faster release of Pb^{2+} . At pH 7, a large amount of PbWO_4 nuclei produced in the solution leads to form very high supersaturation solution, which advantages the formation of HNTs by assembling PbWO_4 nanoparticles. Compared with pH 7.0, the pH 11.0 reaction system provides slow release of Pb^{2+} and at lower Pb^{2+} concentration certain facets to function as a structural directing agent efficiently, resulting in the formation of one-dimensional PbWO_4 nanorods.

In the present work, it is found that the pH value of reaction system has great influence on the morphologies of the obtained samples, when the other conditions were the same. Regarding the formation mechanism of the PbWO_4 nanorods through hydrothermal approach, it is clear that the growth process is not surfactant-assisted or template-directed, because no surfactants or templates are introduced into the reaction system. It is noted from our result that with the increase in pH, the size of PbWO_4 nanoparticles and length of the PbWO_4 nanotubes increases. Morphology changes from HNTs to Nanorods.

4.12 Effect of Synthesis Temperature on Morphology of PbWO_4

Temperature-dependent analysis of TEM images was carried out and they show that reaction temperature is another important parameter that affects the morphology of PbWO_4 samples. We assume that the influence of the temperature on the growth of the PbWO_4 crystals may lie in three aspects similar to pH: affecting the adsorption of surfactant to different facets, changing the relative energy of the different facets, and affecting the controlling growth mechanism.

To investigate the effect of temperature on morphology of undoped PbWO_4 , TEM images of samples prepared at two different reaction temperatures were selected i.e. 100°C and 125°C and TEM photographs of those samples are shown in Figure 4.17 (a-d). As discussed previously, TEM photographs of product obtained at 100°C temperature under identical solution conditions shows mixture of microparticles of octahedral shape having size around 100 nm as well as aggregation of nanoflakes like structure having width 100-150nm and about few μm in length as shown in Figure 4.17(a-b). When the temperature was raised about 125°C , Quasi-spherical hollow nanoparticles having average diameter of about 20-40 nm and Hollow Nano Tubes (HNTs) having outer diameter 12.37 nm and around 80-170 nm in length having uniform smooth surface were obtained which is shown in Figure 4.17(c-d). These HNTs and HNTs are highly crystalline compared to product obtained at 100°C .

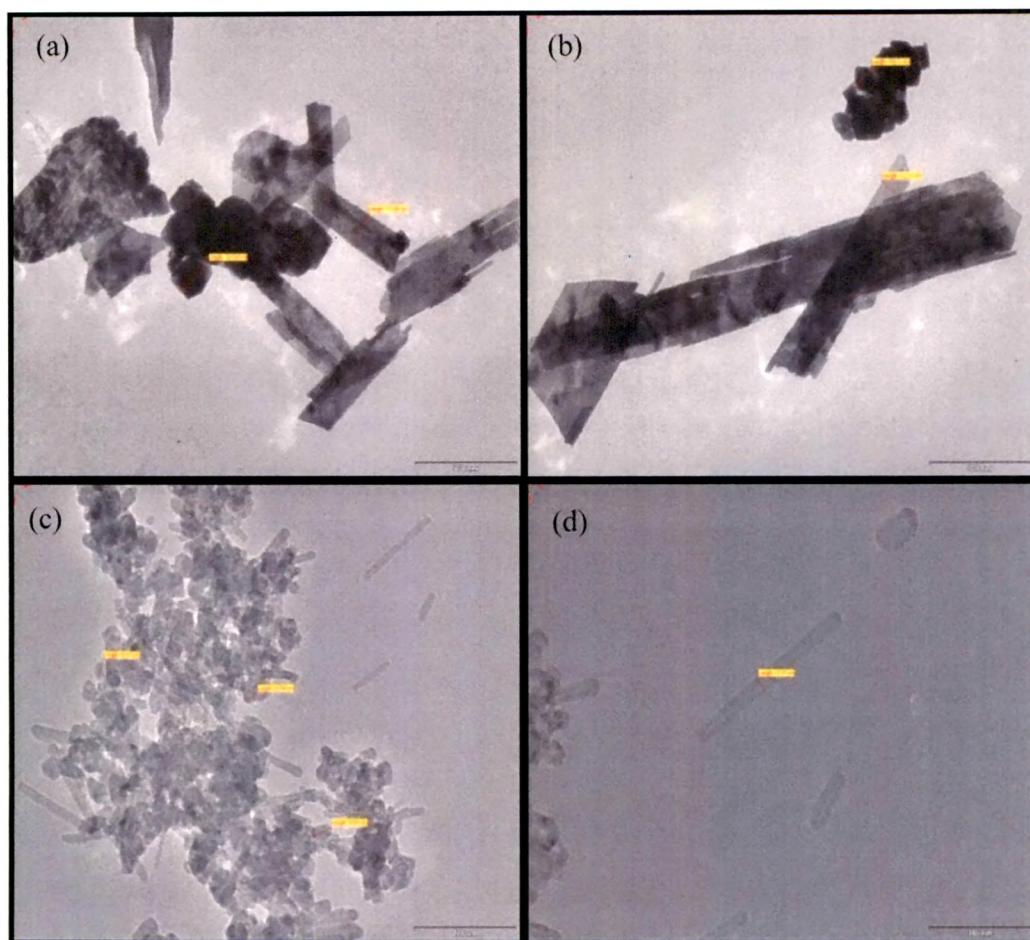


Figure 4.17 TEM images of PbWO_4 prepared at (a-b) 100°C and (c-d) 125°C temperatures.

Xrd analysis of these samples shows that Octahedraon microparticles and nanoflakes obtained at 100°C contains mix phases of stolzite and raspite structures, while Hollow nanoparticles and HNTs produced at 125°C are of pure stolzite phase with high crystallinity. Reasons for production of these morphologies are already discussed in respective sections. Comparison of these products shows that at low temperature (around 100°C), PbWO_4 microstructures containing mix morphologies influenced by raspite as well as stolzite phase will obtained. As we go from low temperature to high temperature raspite phase is diminished and nanostructures with lower dimensions having pure stolzite phase is obtained.

4.13 Effect of Synthesis Temperature on morphology of $\text{PbWO}_4:\text{Ce}$

Temperature-dependent analysis of TEM images was also performed for Cerium doped PbWO_4 samples and it shows that the reaction temperature plays an important role to control the morphology of Cerium doped PbWO_4 samples. To investigate the effect of temperature of reaction solution on the morphology of $\text{PbWO}_4:\text{Ce}$, two reaction temperatures are selected i.e 100°C and 200°C and the TEM photographs of obtained product at these two temperatures are shown in Figure 4.18(a-d).

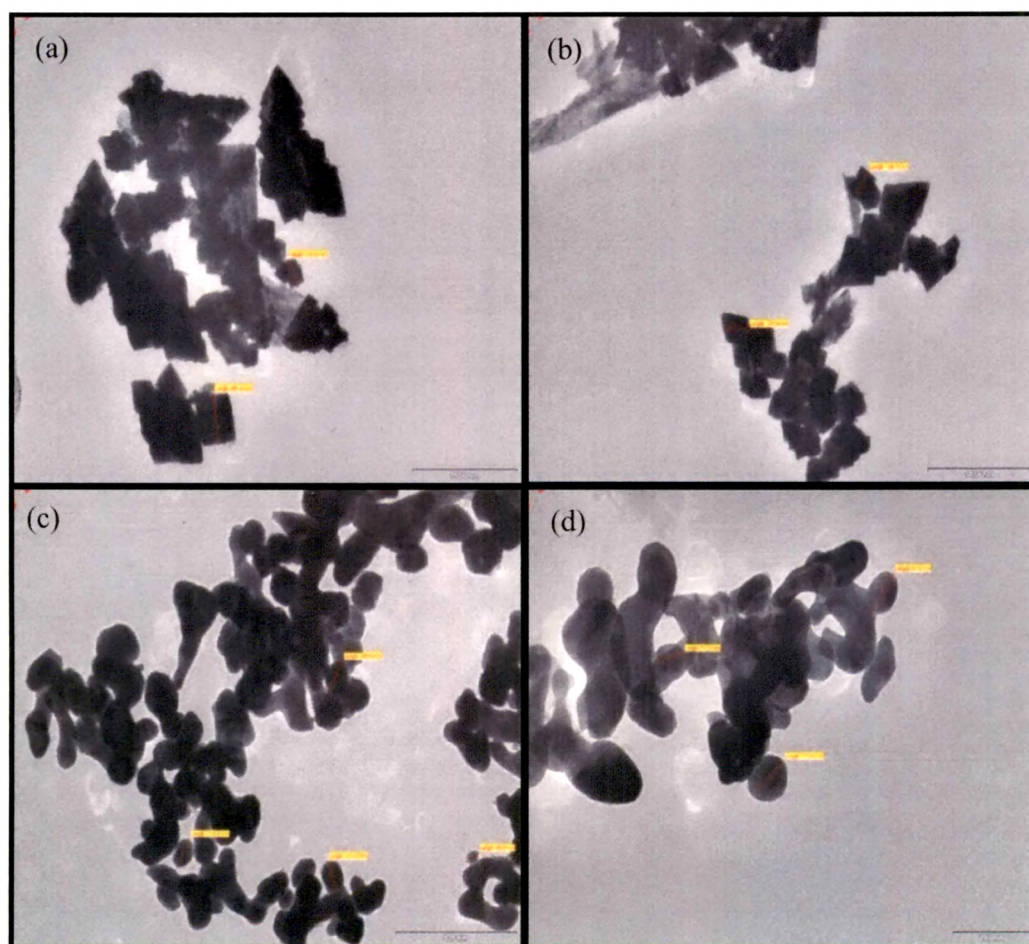


Figure 4.18 TEM images of $\text{PbWO}_4:\text{Ce}$ prepared at (a-b) 100°C and (c-d) 200°C temperatures.

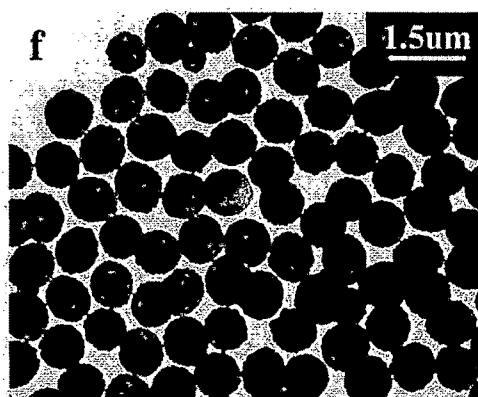


Figure 4.19 TEM image of PbWO_4 microparticle synthesized by hydrothermal method using Tripotassium citrate surfactant at 180°C temperature by Wei Zhao

As discussed previously, doping with cerium in PbWO_4 at 100°C produces tetrahedron microparticles having size around 100 nm as shown in Figure 4.18(a-b). Some inclusions of bamboo-leaf-like morphology also present which can be attributed to raspite phase. PbWO_4 microparticles are attached to each other in an interesting manner. Formation mechanism of this type of dendrite like structure was already explained on the basis of Oswald ripening process followed by oriented attachment of PbWO_4 microparticles to form dendrite. Figure 4.18(c-d) shows the TEM images of Ce doped PbWO_4 synthesized at 200°C temperatures. It is clear from the image that solid spherical nanoparticles are about 50-100 nm in size and they are agglomerated.

X-ray diffraction analysis of these samples shows that Cerium doped PbWO_4 prepared at 100°C contains mix phases of stolzite and raspite structures while spherical nanoparticles prepared at 200°C contains only stolzite phase. The above results indicate that the solution temperature have a certain effect on the morphology along with crystal structure of PbWO_4 . The formation of spherical particles includes the production of nuclei, their growth and finally their stabilization. It was obviously that the sphere-like products were assembled by the nanoparticles obtained initially,

and we considered that the minimization of the surface energy might be the drive force for the formation of spherical PbWO_4 nanoparticles. Figure 4.19 shows the TEM photograph of PbWO_4 microparticle having size about $1\mu\text{m}$ produced by Wei Zhao by hydrothermal method using Tripotassium citrate surfactant at 180°C temperature. These microparticles are composed of PbWO_4 nanorods. Nanospheres obtained in our case (without citrate surfactant) are smaller than that obtained by Wei Zhao. From these results we conclude that raspite phase which exist at low temperature (100°C) vanishes at high temperature (200°C) and to lower the surface energy PbWO_4 with spherical shape forms.

Thus TEM and SEM analysis of our samples shows that different reaction parameters (pH of reaction solution and Temperature) influence the morphologies of PbWO_4 and Cerium doped PbWO_4 to great exchange which is tabulated in Table 4.4.

Table 4.4 Summary of reaction conditions, phase, morphologies and particle size of undoped and Cerium doped PbWO_4 prepared using different Lead chloride.

Sample No.	Temp. (°C)	pH	Phase	Morphology	Dimensions
5	100	7	raspite	micro plates	few μm
			stolzite	micro particles	100nm
6	100	7	stolzite	tetrahedron	100nm
8	125	7	stolzite	Hollow Spherical Nanoparticles (HNPs)	20-40 nm
			stolzite	Hollow Nano Tubes (HNTs)	12.37 nm (OD) 80-170 nm (L)
9	125	11	stolzite	nano rods	40nm (OD) 2 μm (L)
13	200	7	stolzite	spherical nanoparticles	50-100 nm

References

1. D.Tawde, M.Srinivas & K.V.R.Murthy, *Physica Status Solidi A*, Vol.208, Issue 4, 803- 807, 2011.
2. Titipun Thongtem, Sulawan Kaowphong, Somchai Thongtem, *Ceramics International* 35, 1103–1108, 2009.
3. Qilin Dai, Hongwei Song, Xinguang Ren, Shaozhe Lu, Guohui Pan, Xue Bai, Biao Dong, Ruifei Qin, Xuesong Qu and Hui Zhang, *J. Phys. Chem. C*, 112, 19694–19698, 2008.
4. Yan Fang, Ying Xiong ,Yuanlin Zhou , Jinxiang Chen, Kaiping Song, Yi Fang, Xulan Zhen, *Solid State Sciences* 11, 1131–1136, 2009.
5. Jinhu Yang, Conghua Lu, Hong Su, Jiming Ma, Humin Cheng, Limin Qi, *Nanotechnology* 19, 035608, 2008.
6. Thresiamma George, Sunny Joseph, Anu Tresa Sunny, Suresh Mathew, *J Nanopart Res* 10, 567–575, 2008.
7. Chunhua Zheng, Chenguo Hu, Xueyan Chen, Hong liu, Yufeng Xiong, Jing Xu, Buyong Wana and Linyong Huang, *CrystEngComm* 12, 3277–3282, 2010.
8. A. Kashetov and N. A. Gorbatyi, *Russ. Phys. J.*, 20, 860,1969.
9. Biao Liu, Shu-Hong Yu, Linjie Li, Qiao Zhang, Fen Zhang, and Ke Jiang, *Angew. Chem.* 116, 4849–4854, 2004.
10. T. Sugimoto, *Adv. Colloid Interface Sci.* 28,65,1987.
11. J.W. Mullin, *Crystallization*, third ed, Butterworth-Heinemann, Oxford, 1997.
12. Guangjun Zhou , Mengkai Lu, Benyu Su, Feng Gu, Zhiliang Xiu , Shufen Wang, *Optical Materials* 28, 1385–1388, 2006.
13. Guangjun Zhou, MengkaiLu, Feng Gu, Dong Xu, Duorong Yuan , *Journal of Crystal Growth* 276 , 577–582, 2005.
14. Changhua An, Kaibin Tang, Guozhen Shen, Chunrui Wang, Yitai Qian, *Materials Letters* 57, 565– 568, 2002.

15. E. O. Kirkendall, *Trans. AIME*, 147, 104, 1942.
16. A. D. Smigelskas, E. O. Kirkendall, *Trans. AIME*, 171, 130, 1947.
17. H. Nakajima, *J. Miner. Met. Mater. Soc.* 49, 15, 1997.
18. A. Paul, PhD thesis, Technische Universiteit Eindhoven, The Netherlands, 2004.
19. S. Prasad, A. Paul, *Appl. Phys. Lett.*, 90, 233114, 2007.
20. F. Aldinger, *Acta Metal.*, 22, 923, 1974.
21. Q. Li, R. M. Penner, *Nano Lett.*, 5, 1720, 2005.
22. H. J. Fan, M. Knez, R. Scholz, K. Nielsch, E. Pippel, D. Hesse, M. Zacharias, U. Gçsele, *Nat. Mater.*, 5, 627, 2006.
23. H. Tan, S. P. Li, W. Y. Fan, *J. Phys. Chem. B*, 110, 15812, 2006.
24. C. H. B. Ng, H. Tan, W. Y. Fan, *Langmuir*, 22, 9712, 2006.
25. J. Zhou, J. Liu, X. D. Wang, J. H. Song, R. Tummala, N. S. Xu, Z. L. Wang, *Small*, 3, 622, 2007.
26. X. Y. Chen, Z. J. Zhang, Z. G. Qiu, C.W. Shi, X. L. Li, *J. Colloid Interface Sci.*, 308 271, 2007.
27. Y. Chang, M. L. Lye, H. C. Zeng, *Langmuir* 2005, 21, 3746.
28. Q. Wang, J. X. Li, G. D. Li, X. J. Cao, K. J. Wang, J. S. Che, *J. Cryst. Growth*, 299, 386, 2007.
29. C. H. B. Ng, H. Tan, W. Y. Fan, *Langmuir*, 22, 9712, 2006.
30. S.H. Yu, B. Liu, M.S. Mo, J.H. Huang, X.M. Liu, Y.T. Qian, *Adv. Funct. Mater.* 13, 639, 2003.
31. T. Sugimoto, *Photog. Sci. Eng.*, 28, 137, 1984.
32. D.T. Richens, *The Chemistry of Aqua Ions*, Wiley, New York, 1997.
33. G. Zhou, M. Lu", F. Gu, D. Xu, D.R. Yuan, *J. Cryst. Growth* 276, 577, 2005.
34. Peng, Z. A.; Peng, X. G. *J. Am. Chem. Soc.*, 123, 1389, 2001.